Electronic Supplementary Material (ESI) for Nanoscale Horizons.

[Supporting Information]

Nano-crater morphology in hybrid electron-collecting buffer layers for high efficiency polymer:nonfullerene solar cells with enhanced stability

Jooyeok Seo[a], Sungho Nam[ab], Hwajeong Kim*[ac], Donal D. C. Bradley[b], and Youngkyoo Kim*[a]

[1]*Organic Nanoelectronics Laboratory and KNU Institute for Nanophotonics Applications (KINPA), Department of Chemical Engineering, School of Applied Chemical Engineering, Kyungpook National University, Daegu 41566, Republic of Korea*

[2]*Department of Physics, Division of Mathematical, Physical and Life Sciences, University of Oxford, Oxford OX1 3PU, United Kingdom*

[3]*Priority Research Center, Research Institute for Environmental Science & Technology, Kyungpook National University, Daegu 41566, Republic of Korea*

*All correspondences to: Prof. Y. Kim

Email) ykimm@knu.ac.kr, Tel) +82-53-950-5616

EXPERIMENTAL METHODS

***Materials and Solutions*:** PBDB-T (number-average molecular weight = 18 kDa, polydispersity index = 2.5), ITIC and IT-M were used as received from Solarmer Materials Inc. (China). PEOz (weight-average molecular weight = 50 kDa, polydispersity index = 3 ~ 4), zinc acetate dihydrate, ethanolamine, and 2-methoxyethanol were purchased from Sigma-Aldrich (USA). The ZnO precursor solutions were prepared by dissolving zinc acetate dihydrate (100 mg) in 2-methoxyethanol (1 ml) in the presence of ethanolamine (28 μl), followed by addition of PEOz (0~20 wt% to the amount of zinc acetate dihydrate). These solutions were stirred for reactions at 60 ^{o}C for 4 h and then at room temperature for a day. Binary solutions of PBDB-T and ITIC were prepared using chlorobenzene (solvent) in the presence of 1,8-diiodooctane (chlorobenzene:1,8-diiodooctane = 99:1 by volume) at a solid concentration of 20 mg/ml (PBDB-T:ITIC = 1:1 by weight ratio), which were subjected to vigorous stirring at 50 ^{o}C for more than a day.

***Film and Device Fabrication*:** Indium-tin oxide (ITO)-coated glass substrates (sheet resistance = 12 Ω/cm^2) were patterned using photolithography/etching processes in order to make the ITO electrodes for inverted-type solar cells. The patterned ITO-coated substrates were cleaned using acetone and isopropyl alcohol in an ultrasonic cleaner (CPX5800H-E, Branson), followed by drying under a nitrogen flow. The wet-cleaned ITO-coated substrates were further treated with UV-ozone for 20 min by employing a UV ozone cleaner (AC-6, Ahtech LTS). Next, the ZnO:PEOz precursor films were spin-coated on the UV-ozone-treated ITO-coated substrates, followed by thermal annealing at 150 ^{o}C for 1 h in an air ambient dark condition. After thermal annealing, the samples were transferred to a nitrogen-filled glove box for active layer coating processes. The PBDB-T:ITIC layers were spin-coated on the sol-gel processed ZnO:PEOz hybrid layers at 2500 rpm for 60 s and thermally annealed at 100 ^{o}C for 15 min inside the same glove box. The final thickness of the PBDB-T:ITIC layers was about 100 nm. The active layer-coated samples were moved to a vacuum chamber equipped inside an argon-filled glove box. After reaching a working pressure of ca. 1 x 10^{-6} torr, MoO_3 (10 nm) and silver (Ag, 80 nm) were sequentially deposited on the PBDB-T:ITIC layers through a shadow mask by thermal evaporation. The active area of all devices was fixed to 0.05 cm^2. Note that the electron-only devices for the hybrid electron-collecting buffer layers were fabricated by sequential deposition of lithium fluoride (LiF, ~1 nm) and aluminum (Al, 90 nm), leading to glass/ITO/ZnO:PEOz/LiF/Al, in the same vacuum chamber.

***Measurements*:** The thickness of each layer was measured by employing a surface profilometer (Alphas Step 200, Tencor Instruments). The optical transmittance and absorption spectra of

samples were measured using a UV-visible spectrometer (Optizen 2120, MECASYS). The work functions of the pristine ZnO and hybrid electron-collecting buffer layers were measured using a Kelvin probe (KP) system with a gold tip of 2 mm diameter (APS01, KP Technology), which was installed inside a nitrogen-filled glove box, and were calibrated with a highly ordered pyrolytic graphite. An optical microscope (SV-55, Sometech) was used to inspect the quality of all film samples on a micrometer scale. The surface morphology of hybrid electron-collecting buffer layers was examined by employing a field-emission scanning electron microscope (FESEM, S-4800, Hitachi) and an atomic force microscope (AFM, Nanoscope IIIa, Digital Instruments). The atom (carbon) distribution images near the surface region (maximum penetration depth = 5.5 nm) were measured with an Auger electron microscope (AEM, PHI700TM, Physical Electronics), while the atom (Zn) distribution images for the cross-section parts of devices were measured using a scanning transmission electron microscope (Titan G2 ChemiSTEM Cs Probe, FEI Company) after manipulating the samples with a focused ion beam (FIB) system (Versa3D LoVac, FEI Company). The core-level atom environments (N1s and O1s) were measured using an X-ray photoelectron spectrometer (XPS, ESCALAB 250Xi, Thermo Scientific, Inc.) with a penetration depth of ca. 5 nm. The J-V curves of electron-only devices were measured under dark in a nitrogen atmosphere using an electrometer (Keithley 2400, Keithley Instruments). The performance of solar cells was measured using a solar cell measurement system equipped with a solar simulator (class-A, 92250A-1000, Newport-Oriel) and an electrometer (Keithley 2400). The intensity (100 mW/cm^2) of simulated solar light from the solar simulator was adjusted with a calibrated standard solar cell (BS-520, Bunkoukeiki Co., Ltd) that is accredited by the Advanced Institute of Science and Technology (AIST, Japan), while the active area was exactly exposed to the simulated solar light. The external quantum efficiency (EQE) spectra of solar cells were measured using a specialized EQE measurement system equipped with a monochromator (CM110, Spectral Products) and a light source (Tungsten-Halogen lamp, 150 W, ASBN-W, Spectral Products). The short circuit current density from the light J-V curves was compared with the integrated current density calculated from the EQE spectra in order to avoid any possible overestimation caused by a waveguide effect etc. The series (R_S) and shunt (R_{SH}) resistances were calculated by $R_S = \frac{\Delta V}{\Delta J}$ at around open circuit condition and $R_{SH} = \frac{\Delta V}{\Delta J}$ at around short circuit condition, respectively.[39] The brief lifetime test was performed using the same solar simulator, while the solar cells were mounted inside a nitrogen-filled sample holder during the lifetime test. The electron mobility was obtained by measuring the J-V curves of electron-only devices (glass/ITO/ZnO:PEOz/LiF/Al)

under forward bias condition because only electrons can be injected from the Al electrodes to the ZnO:PEOz layers without any hole injection from the ITO electrode owing to the huge energy barrier (ca. 2.6 eV).

Table S1. Summary of glass transition temperature (Tg) for various plastic film substrates.

Flexible Substrates	Tg (°C)	References
PSO (Polysulfone)	190	https://www.solvay.com/en/binaries/Membranes-Processing-Guide_EN-228113.PDF
PES (Poly(ether sulfone))	185	http://www.allsealsinc.com/05_Plastic-Thermoplastic.pdf
COP (Cyclic Olefin Polymer)	178	https://www.polyplastics.com/en/product/lines/topas/general_e.pdf
PEEK (Poly(ether ether ketone))	153	A. Reyna-Valencia *et al.*, J. Appl. Polym. Sci. **99**, 756 (2006)
PC (Polycarbonate)	150	E. S. Mast *et al.*, Smoothing and barrier layers on high Tg substrates**,** US Patent 09/553,191 (2000)
PEN (Poly(ethylene naphthalate))	120	http://www.aimcal.org/uploads/4/6/6/9/46695933/lariviere_pres.pdf

Table S2. Summary of recent reports on the correlation between work function (WF) shift and open circuit voltage (V_{OC}) increase.

WF Shift (meV)	V_{OC} Increase (meV)	References
500	40 (0.66 V → 0.70 V)	H. Kang *et al*., Adv. Mater. **24**, 3005 (2012)
350	20 (0.71 V → 0.73 V)	F. Liu *et al*., Adv. Mater. **25**, 6868 (2013)
240	20 (0.71 V → 0.73 V)	S. Woo *et al*., Adv. Energy Mater. **4**, 1301692 (2014)
160	10 (0.79 V → 0.80 V)	S.-H. Liao *et al*., Sci. Rep. **4**, 6813 (2014)
100	20 (0.62 V → 0.64 V)	S.-H. Oh *et al*., Adv. Funct. Mater. **20**, 1977 (2010)
80	6 (0.749 V → 0.755 V)	Z.-G. Zhang *et al*., Energy Environ. Sci. **7**, 1966 (2014)
50	20 (0.76 V → 0.78 V)	M. Lv *et al*., Adv. Mater. **25**, 6889 (2013)
40	4 (0.949 V → 0.953 V)	X. Li *et al*., Chem. Mater. **29**, 4176 (2017)

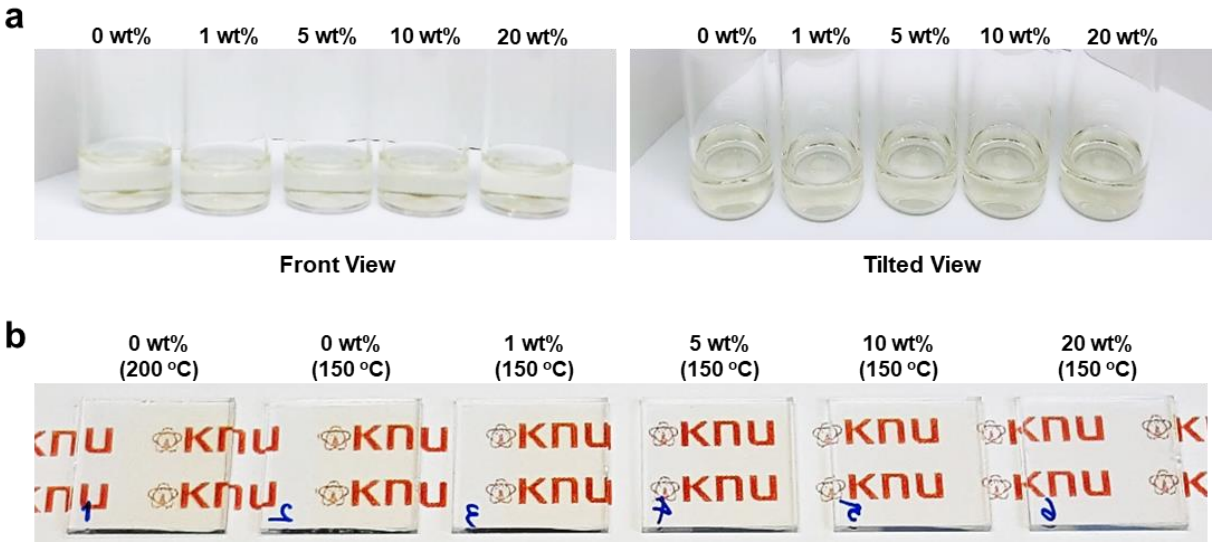

Fig. S1. Photographs for solutions and films. a, ZnO:PEOz hybrid precursor solutions according to the PEOz content (left: front view, right: tilted view). **b,** Pristine ZnO and ZnO:PEOz hybrid films (layers) coated on the ITO-glass substrates. Note that all solutions were optically clear and resulting films showed high optical transparency.

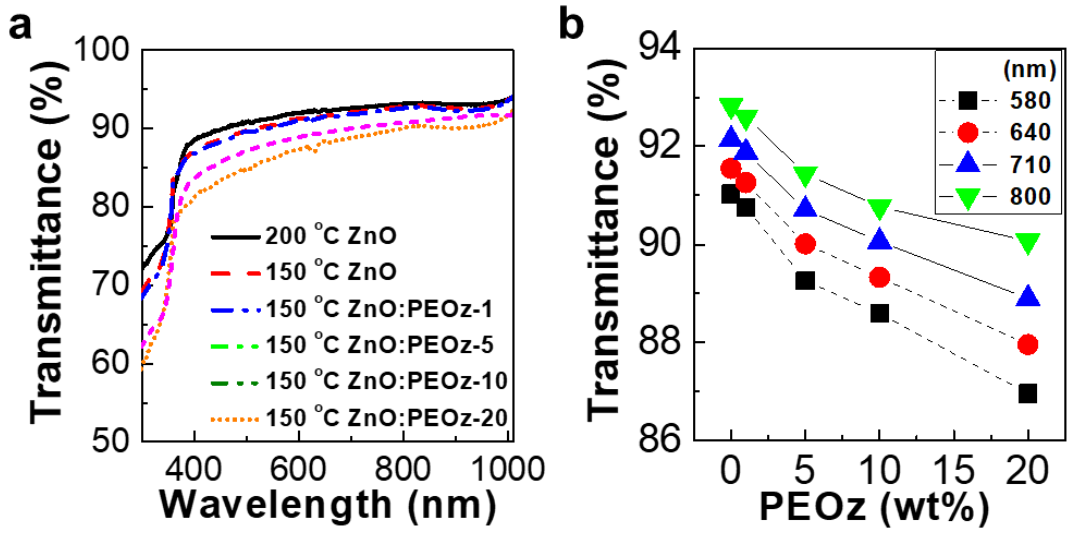

Fig. S2. Optical transmittance spectra of films. a, Optical transmittance spectra for the pristine ZnO and ZnO:PEOz hybrid films coated on the ITO-glass substrates: ZnO:PEOz-1, ZnO:PEOz-5, ZnO:PEOz-10, and ZnO:PEOz-20 denote corresponding hybrid films with the PEOz content of 1, 5, 10, and 20 wt%. **b,** Optical transmittance at a fixed wavelength (580, 640, 710, and 800 nm) as a function of the PEOz content.

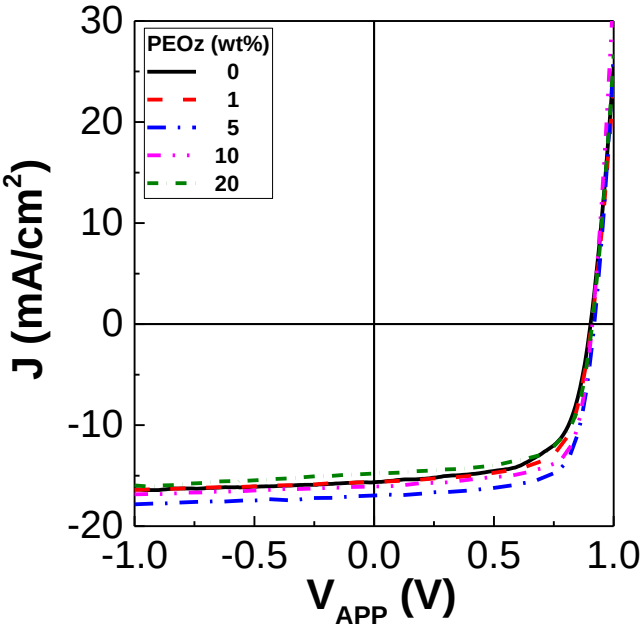

Fig. S3. Full-scale light (air mass 1.5G, 100 mW/cm^2) J-V curves for the inverted-type PBDB-T:ITIC solar cells with the ZnO:PEOz hybrid layers annealed at 150 ºC.

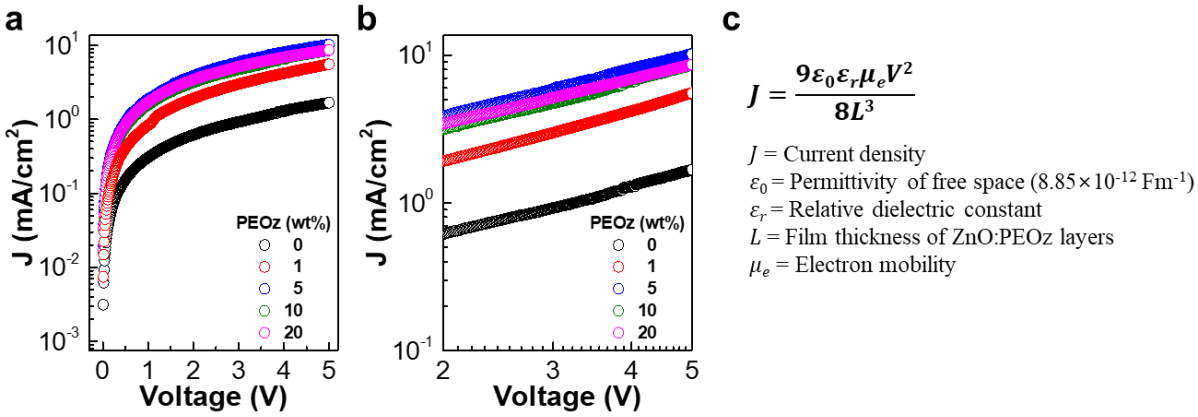

Fig. S4. Electrical characteristics of electron-only devices (structure = glass/ITO/ZnO:PEOz/LiF/Al). a, Current density – voltage (J-V) curves for the electron-only devices on a semi-logarithmic scale. **b**, J-V curves for the electron-only devices on a double logarithmic scale in the voltage range of space-charge-limited current (SCLC) regime. **c,** Equation for the calculation of SCLC electron mobility.

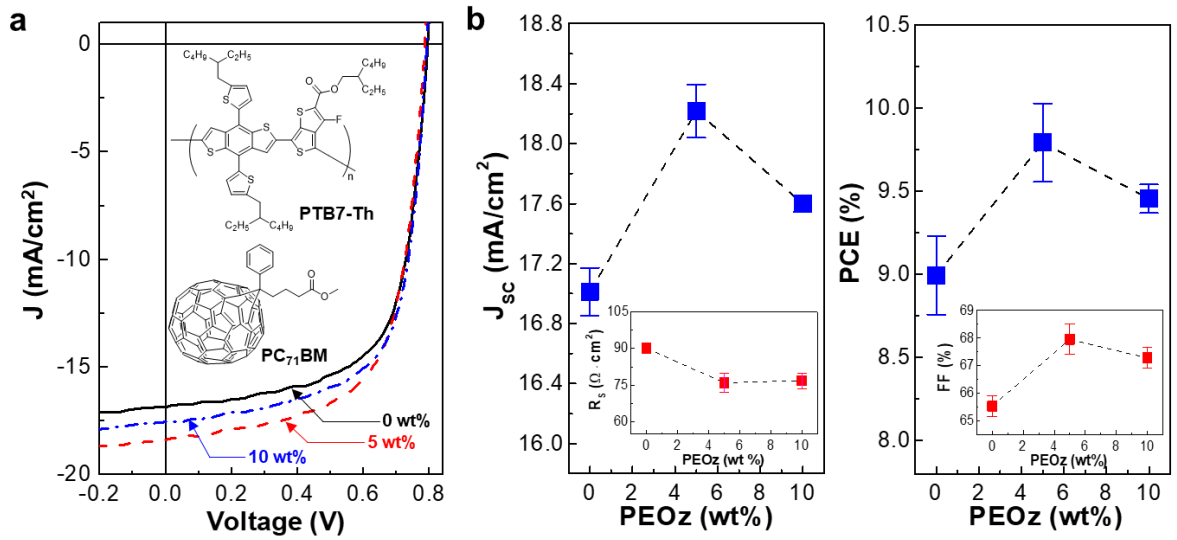

Fig. S5. Performance of polymer:fullerene solar cells. a, Light (air mass 1.5G, 100 mW/cm^2) J-V curves for the inverted-type PTB7-Th:$PC_{71}BM$ solar cells with the ZnO:PEOz hybrid layers annealed at 150 ºC. **b,** Solar cell parameters as a function of the PEOz content.

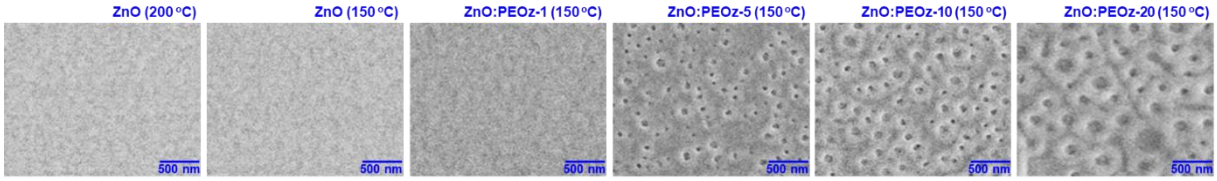

Fig. S6. SEM images for the pristine ZnO (200 ºC, 150 ºC) and ZnO:PEOz hybrid films according to the PEOz content. The nano-craters can be clearly seen from the PEOz content of 5 wt%.

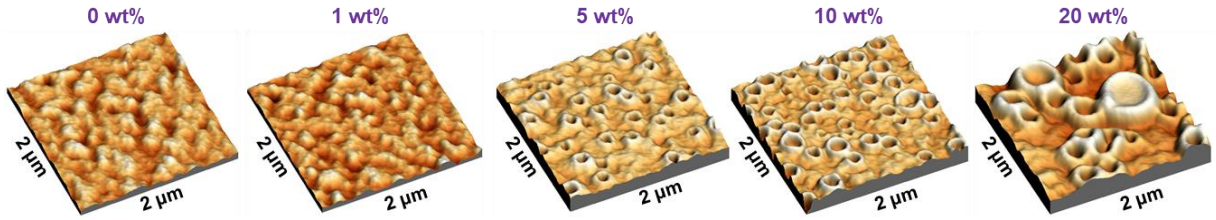

Fig. S7. 3D height-mode AFM images for the pristine ZnO (150 ºC) and ZnO:PEOz hybrid films according to the PEOz content. The nano-craters can be clearly seen from the PEOz content of 5 wt%, while the number of nano-craters was higher for 10 wt% than 5 wt%.

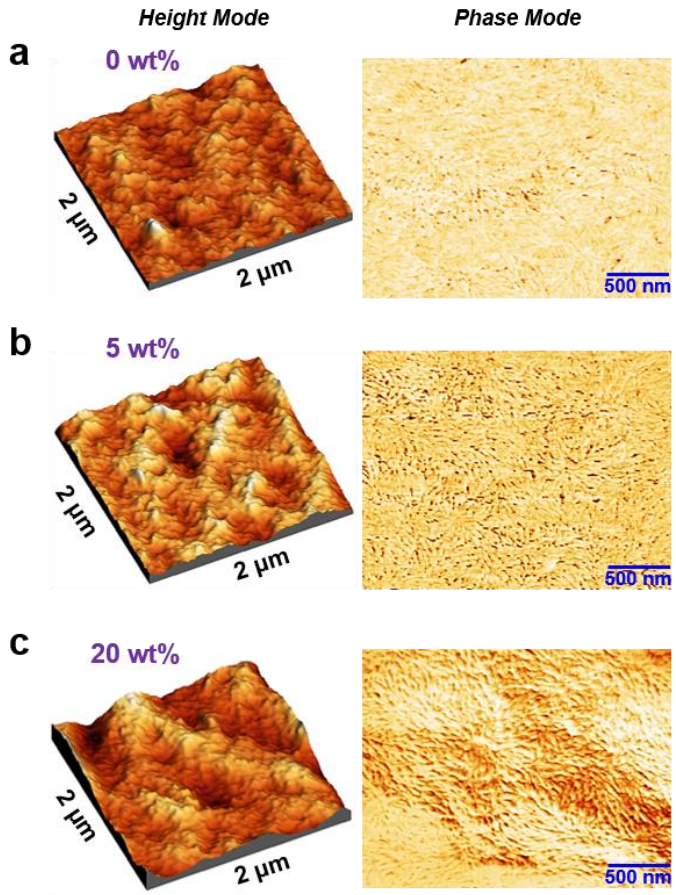

Fig. S8. 3D height-mode (left) and phase-mode (right) AFM images for the PBDB-T:ITIC BHJ layers. a, BHJ layer coated on the pristine ZnO layer (annealed at 150 ºC). **b,** BHJ layer coated on the ZnO:PEOz-5 hybrid layer (annealed at 150 ºC). **c,** BHJ layer coated on the ZnO:PEOz-20 hybrid layer (annealed at 150 ºC).

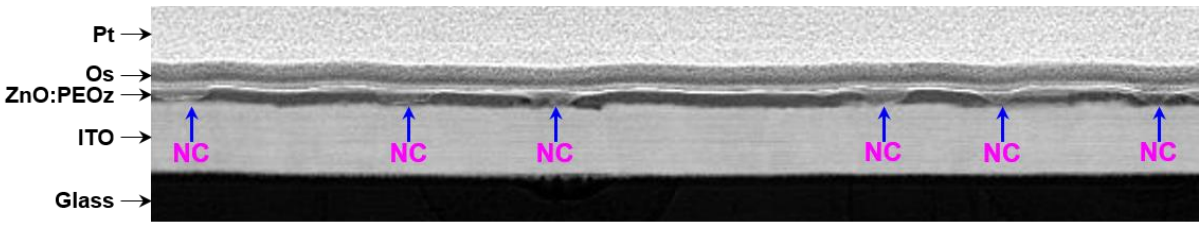

Fig. S9. HRTEM image for the cross-section part of the ZnO:PEOz-5 hybrid layer coated on the ITO-glass substrates. The position of nano-craters is marked with 'NC'. Note that the cross-section part of samples was prepared by employing the focused ion beam (FIB) technique. Note that the empty-like bottom part of some nano-craters could be caused by the breaking during the FIB process.

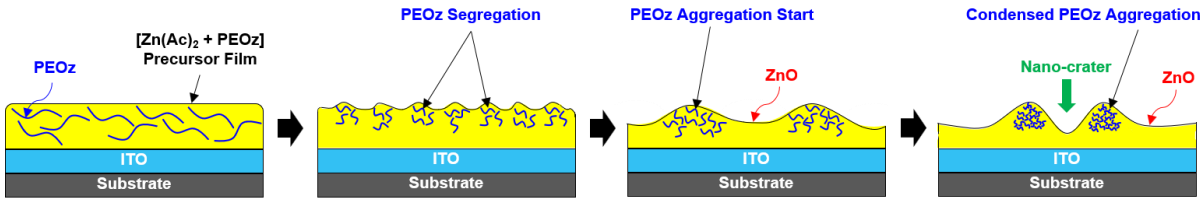

Fig. S10. A mechanism proposed for the formation of nano-craters in the ZnO:PEOz hybrid layers. The initial phase segregation between ZnO precursors and PEOz chains is considered to extend to the phase aggregation and finally leading the condensed PEOz aggregates in the solid-sate hybrid layers.

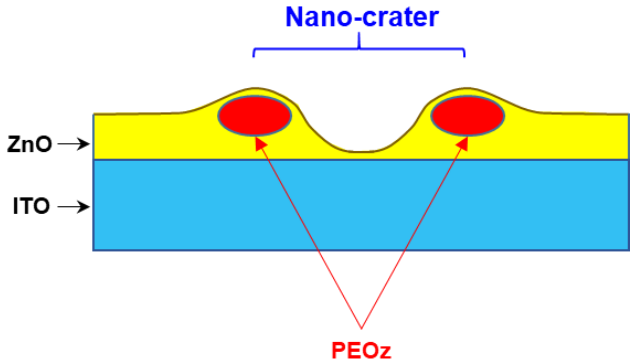

Fig. S11. A proposed cross-section view for the nano-crater in the ZnO:PEOz hybrid layers coated on ITO-glass substrates. The position of PEOz was assumed according to the AEM and XPS measurement results. Note that the surface area (A_{SNC}) for the ZnO:PEOz hybrid layers (5 wt% PEOz) was calculated on the basis of 2 μm × 2 μm AFM images in Fig. S7 as follow: Both AFM image and proposed cross-section view here provide the radius (r = 75 nm) and number (n = 30 in the area of 2 μm × 2 μm) of nano-craters. The flat area (A_F) of one nano-crater is obtained from $A_F = \pi r^2 = 1.77\times10^{-10}$ cm^2, while the surface area (A_{SH}) of one hemisphere (nano-crater) is calculated by $A_{SH} = 3\pi r^2$ ($= \pi r^2 + 2\pi r^2$) $= 5.31\times10^{-10}$ cm^2. Assuming that the surface area without nano-craters (A_{S0}) is simply the size of AFM image (A_{S0} = 2 μm × 2 μm = 4.0×10^{-8} cm^2), the surface area with the nano-craters (A_{SNC}) is obtained from $A_{SNC} = A_{S0} - n\times A_F + n\times A_{SH} = 4.0\times10^{-8}$ cm^2 – 30 × (1.77×10^{-10} cm^2) + 30 × (5.31×10^{-10} cm^2) = 5.062×10^{-8} cm^2. Therefore, it is concluded that the surface area was increased by ca. 27 % (from 4.0×10^{-8} cm^2 to 5.062×10^{-8} cm^2) after forming the nano-craters.

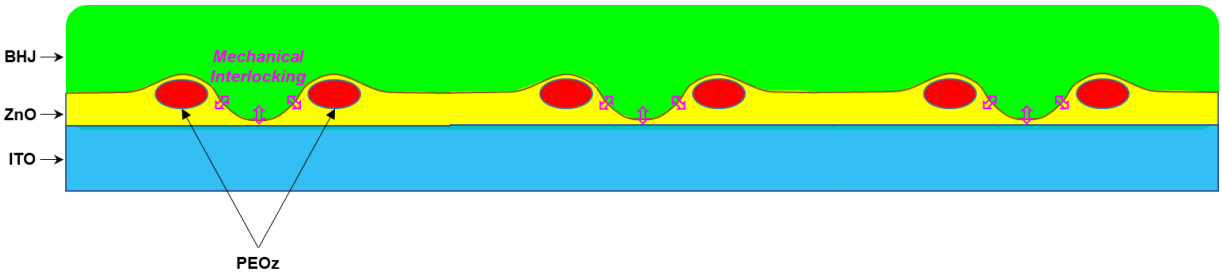

Fig. S12. Illustration for the possible mechanical interlocking due to the semi-interdigitated structure formed by the nano-crater morphology between the BHJ (PBDB-T:ITIC) layer and the ZnO:PEOz hybrid layer.

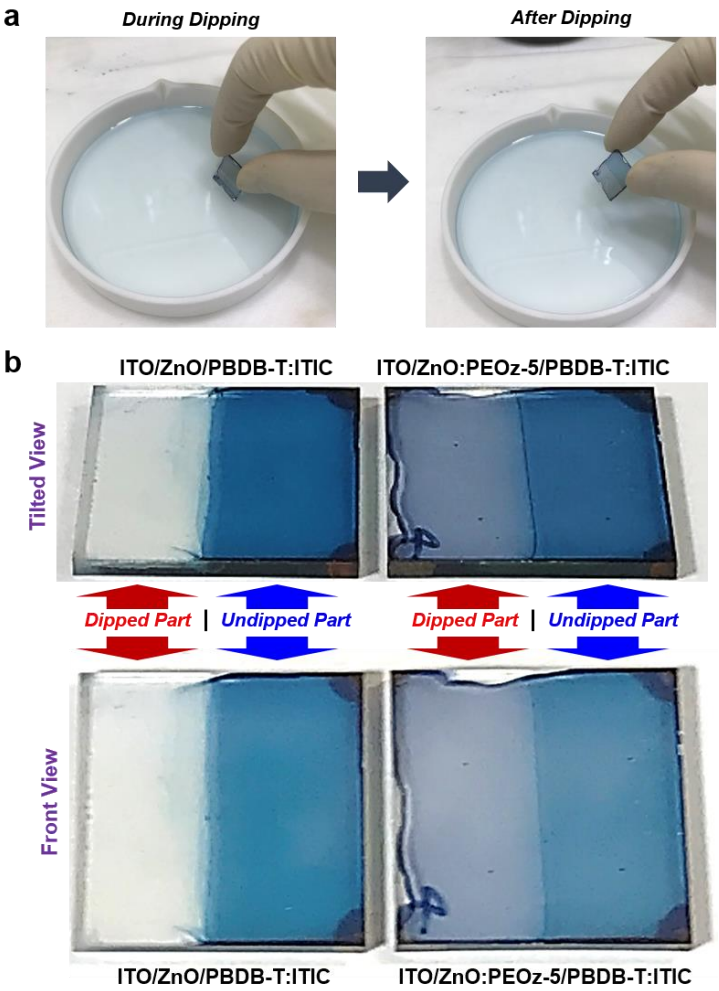

Fig. S13. Dissolution test in chlorobenzene for the BHJ (PBDB-T:ITIC) films, which are coated on the pristine ZnO layer or the ZnO:PEOz hybrid layer prepared on the ITO-glass substrates, to examine the effect of mechanical interlocking structures. **a,** Photographs before and after dipping the half part of the sample (BHJ film coated on the ZnO:PEOz-5 hybrid layer) in chlorobenzene. **b,** Photographs for the samples after dipping in chlorobenzene for 2 s: (left) glass/ITO/ZnO/PBDB-T:ITIC, (right) glass/ITO/ZnO:PEOz-5/PBDB-T:ITIC. Note that the dipped part was almost completely removed in the case of the pristine ZnO layer. However, the considerable amount of the dipped part was still maintained in the case of the ZnO:PEOz-5 hybrid layer, which indicates strong adhesion of the BHJ layer on the ZnO:PEOz-5 layer due to the formation of mechanical interlocking structures.

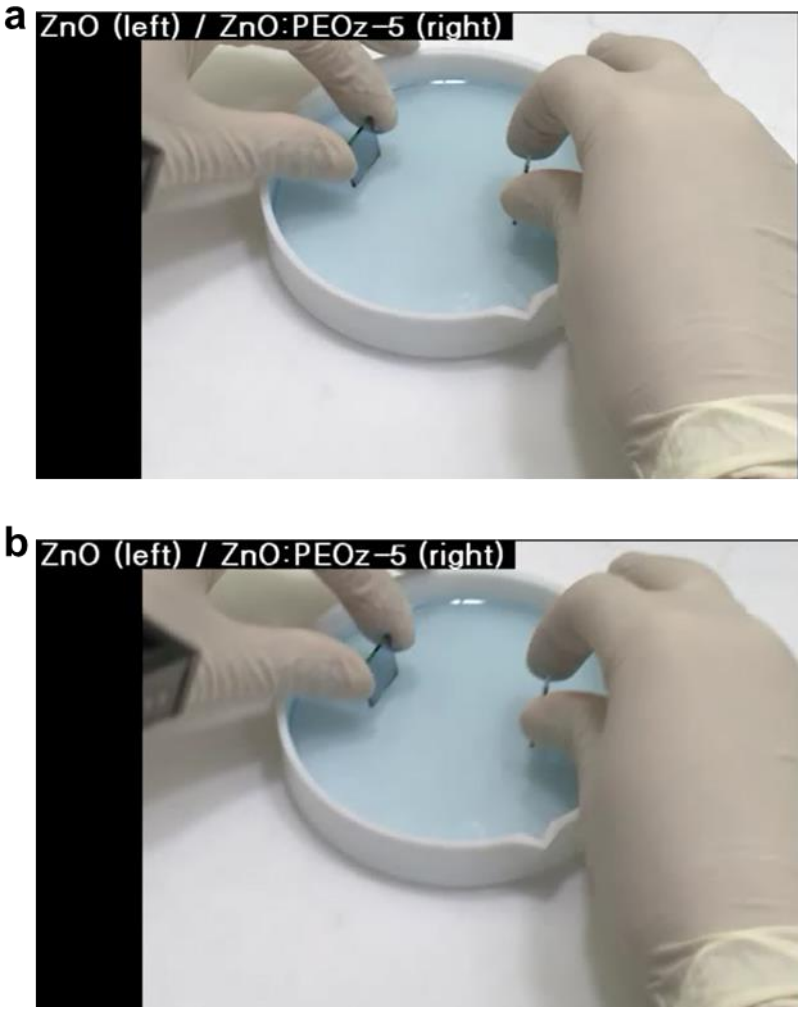

Fig. S14. Video clips for the dissolution test in chlorobenzene for the BHJ (PBDB-T:ITIC) films, which are coated on the pristine ZnO layer or the ZnO:PEOz hybrid layer prepared on the ITO-glass substrates. **a**, No nitrogen blowing to dry the solvent from the samples after taking out (filename: Fig_S14a_No Nitrogen Blowing). **b**, Nitrogen blowing to dry the solvent from the samples after taking out (filename: Fig_S14b_Nitrogen Blowing).